

Intriguing roles of reactive intermediates in dissociation chemistry of *N*-phenylcinnamides†Cheng Guo,^a Kezhi Jiang,^b Lei Yue,^a Ziming Xia,^c Xiaoxia Wang^c and Yuanjiang Pan^{*a}

Received 24th May 2012, Accepted 11th July 2012

DOI: 10.1039/c2ob26011e

In mass spectrometry of protonated *N*-phenylcinnamides, the carbonyl oxygen is the thermodynamically most favorable protonation site and the added proton is initially localized on it. Upon collisional activation, the proton transfers from the carbonyl oxygen to the dissociative protonation site at the amide nitrogen atom or the α -carbon atom, leading to the formation of important reactive intermediates. When the amide nitrogen atom is protonated, the amide bond is facile to rupture to form ion/neutral complex **1**, [RC₆H₄CH=CHCO⁺/aniline]. Besides the dissociation of the complex, proton transfer reaction from the α -carbon atom to the nitrogen atom within the complex takes place, leading to the formation of protonated aniline. The presence of electron-withdrawing groups favored the proton transfer reaction, whereas electron-donating groups strongly favored the dissociation (aniline loss). When the proton transfers from the carbonyl oxygen to the α -carbon atom, the cleavage of the C _{α} -CONHPh bond results in another ion/neutral complex **2**, [PhNHCO⁺/RC₆H₄CH=CH₂]. However, in this case, electron-donating groups expedited the proton transfer reaction from the charged to the neutral partner to eliminate phenyl isocyanate. Besides the cleavage of the C _{α} -CONHPh bond, intramolecular nucleophilic substitution (a nucleophilic attack of the nitrogen atom at the β -carbon) and stepwise proton transfer reactions (two 1,2-H shifts) also take place when the α -carbon atom is protonated, resulting in the loss of ketene and RC₆H₅, respectively. In addition, the H/D exchanges between the external deuterium and the amide hydrogen, vinyl hydrogens and the hydrogens of the phenyl rings were discovered by D-labeling experiments. Density functional theory-based (DFT) calculations were performed to shed light on the mechanisms for these reactions.

Introduction

Protonation has long been recognized as a fundamental process that plays an important role in many chemical and biological reactions.^{1–5} For molecules with multiple functional groups, protonation may take place at different sites, resulting in different forms of protonated molecules. The thermodynamically favored site of protonation is mainly dependent on the proton affinity (PA)⁶ at each local functionality of the molecule. However, it has been revealed that the chemical environment, such as solvent^{7–9}

or a neighboring group^{10–12} also influences the site of protonation.

Mass spectrometry (MS) has become an invaluable tool for fundamental studies of protonation of molecules in the gas phase. Information on how a molecule is protonated is important for structural elucidation using electrospray ionization (ESI) mass spectrometry where the molecules of interest are protonated. It is common that the cleavage of protonated molecules is triggered by the positive charge derived from protonation.¹³ However, it is often found that when the molecule is protonated at the thermodynamically favored site, no fragmentation takes place. In contrast, the fragmentation reaction occurs when the proton transfers to some unfavorable sites. These less favored protonation sites were recently described as the dissociative protonation sites,¹⁴ which are the reactive centers in ESI-MS.^{15–20}

Many types of reactive intermediates such as σ -, π -, or proton-bonded complexes have been invoked in the unimolecular reactions of organic ions in the gas phase. Another interesting and important intermediate is the non-traditional ion/neutral complex (INC),^{21–30} which is composed of a charged fragment and a neutral species that are held together by electrostatic forces but

^aDepartment of Chemistry, Zhejiang University, Zheda Road No. 38, Hangzhou 310027, China. E-mail: panyuanjiang@zju.edu.cn; Fax: +86-571-87951629; Tel: +86-571-87951264

^bKey Laboratory of Organosilicon Chemistry and Material Technology, Hangzhou Normal University, Hangzhou, 310012, China

^cCollege of Chemistry and Life Sciences, Zhejiang Normal University, Jinhua 321004, China

† Electronic supplementary information (ESI) available: NMR spectra of key compound, Cartesian coordinates, total energies, zero point energy corrections and the number of imaginary frequencies of the structures discussed in the text. See DOI: 10.1039/c2ob26011e

still maintain their individual mobility. Before the final departure, a variety of interesting chemical reactions may take place between the two partners or in the ionic fragment alone. As a matter of fact, it is more than five decades since Meyerson and Rylander involved ion/neutral complex to elucidate the loss of identity of labels in the benzyl ions produced from *tert*-butylbenzene.³¹ Since that time, the concept of INC has widely been utilized to explain a number of otherwise puzzling ionic reactions in the gas phase.

The gas phase chemistry of amides is of great interest because the amide bond not only forms the fundamental linkage between monomeric amino acid residues in peptides and proteins but also is an important functional group in many drug molecules. In the past few decades, a tremendous amount of effort has been made to determine the thermodynamically favored site of protonation and it has been agreed that the amides are protonated preferentially at the carbonyl oxygen in most cases.^{32–34} However, the major fragmentation reaction of protonated amides in mass spectrometry is the cleavage of the amide bond resulting in the loss of the amine or ammonia, which requires the amide nitrogen to be protonated. From the initial stable *O*-protonated species to the less stable dissociative *N*-protonated isomer, a 1,3-proton transfer prior to the fragmentation is necessary even though the energy of the *N*-protonated molecule is higher than that of the *O*-protonated one and a high energy barrier exists between the two isomeric forms. For instance, a combined theoretical and experimental investigation of formamide³⁵ has revealed that the energy difference between the two isomers is 14.3 kcal mol^{−1} and the energy barrier of the 1,3-proton transfer is 69.1 kcal mol^{−1}. This has led to the proposal of the mobile proton model^{36–39} which describes the mobility of the proton across the protonated molecule and is applied to the flexible peptides and proteins besides the rigid molecules.

Dissociative protonation plays an important role in the fragmentation of many drug molecules. For example, the fragmentation of the protonated penicillins which contain two amide bonds is dominated by cleavage of the β -lactam bond^{40,41} and requires protonation at the lactam nitrogen. For conjugated amides, protonation at the α -carbon is required for the cleavage of the C $_{\alpha}$ –CONHR bond. As a typical example, atorvastatin, which is a drug for the treatment of high serum cholesterol, has a phenylamido moiety conjugated with the central pyrrole ring. In the CID mass spectrum of its [M + H]⁺ ion (*m/z* 559), the base peak is observed at *m/z* 440,^{42,43} corresponding to loss of phenyl isocyanate (O=C=NC₆H₅). What these observations reflect is the fact that the arrival of the proton at a dissociative site of the molecule is required for the fragmentation reaction.

Recently, *N*-phenylcinnamides, have been reported to be novel antimitotic agents which are an especially important class of anticancer drugs.⁴⁴ Mass spectrometry, due to its capability of providing both molecular weight and abundant structural information, has been routinely employed in the realm of drug discovery. In mass spectrometry of protonated *N*-phenylcinnamides, the proton migrates from the thermodynamically favored site at the carbonyl oxygen to the dissociative protonation site at the amide nitrogen or the α -carbon leading to the formation of important intermediates. Many interesting reactions such as proton transfer and intramolecular nucleophilic substitution (S_NI)

mediated by these reactive intermediates have been discovered and investigated in the present study.

Experimental

Materials

The *N*-phenylcinnamides were synthesized following the procedures described in the literature⁴⁴ using the corresponding carboxylic acid and aniline. The structures were confirmed using ¹H NMR, ¹³C NMR and HRMS after the purification of the crude products. *N*-Phenylcinnamide (compound 1), ¹H NMR (CDCl₃, 500 MHz): δ 8.62 (s, 1H), 7.63–7.60 (m, 3H), 7.25–7.24 (m, 2H), 7.19–7.16 (m, 3H), 7.14–7.11 (m, 2H), 6.98 (t, 1H, *J* = 7.5 Hz), 6.64 (d, 1H, *J* = 15.5 Hz); ¹³C NMR (CDCl₃, 125 MHz): δ 165.0, 142.3, 138.4, 134.8, 130.0, 129.2, 128.9, 128.1, 124.6, 121.4, 120.6; HRMS calcd for C₁₅H₁₄ON⁺ ([M + H]⁺): 224.1070, found: 224.1071.

Mass spectrometry

The collision-induced dissociation experiments were performed on a Varian 500-MS ion trap mass spectrometer equipped with an electrospray ionization (ESI) source in positive ion mode, with data acquisition using the Varian MS Workstation (Varian, Palo Alto, CA, USA). The compounds were dissolved in 1 : 1 CH₃OH : 1% aqueous formic acid. And methanol-d₄ was used as solvent for the D-labeling experiment. The samples were infused into the source chamber at a flow rate of 10 μ L min^{−1} with parameters: spray chamber temperature, 50 °C; needle voltage, 5000 V; spray shield voltage, 600 V; capillary voltage, 80 V; RF loading, 70%; scan mode, standard; drying gas temperature, 350 °C. Nitrogen was used as the drying gas at a pressure of 10 psi and the nebulizing gas at a pressure of 30 psi. Tandem mass spectra were obtained by CID with helium as the collision gas after isolation of the desired precursor ion and the isolation window was set as 1.0 *m/z* unit. The collision energy (resonance mode) was set at 0.50 V to give suitable energy for the dissociation of all compounds.

All accurate mass spectrometric experiments were carried out on an Apex III (7.0 Tesla) FTICR mass spectrometer (Bruker, Billerica, MA, USA). XMASS software version 6.1.1 (Bruker) was used for instrument control, data acquisition and processing. Sodium trifluoroacetate was used as an external calibration compound. Solutions were infused from the ESI source at 3 μ L min^{−1} with the following parameters applied: capillary, −4448 V; end plate, −4233 V; skimmer 1, 12.00 V; skimmer 2, 6.61 V; offset, 0.98 V; RF amplitude, 582.5 Hz; drying gas temperature, 150 °C. Nitrogen was used as the nebulizing and drying gas, and argon was used as the collision gas. MS/MS analysis was performed through isolation of the desired precursor ion using a correlated sweep. Sustained off-resonance irradiation (SORI) was applied for CID. The pulse parameters were set as follows: correlation sweep pulse length, 1000 μ s; correlation sweep attenuation, 19 dB; ejection safety belt, 1000 Hz; ion activation pulse length, 250 000 μ s; ion activation attenuation, 49.5 dB; frequency offset from activation mass, 600 Hz; user delay length, 3 s.

Theoretical calculations

All theoretical calculations were performed by using the DFT method at the RB3LYP/6-31G(d) level of theory in the Gaussian 03 program.⁴⁵ The candidate structures of the reactants, products, intermediates and transition states were optimized by calculating the force constants. No symmetry constraints were imposed in the optimizations. The reaction pathways were traced forward and backward by the intrinsic reaction coordinate (IRC) method. All optimized structures were subjected to vibrational frequency analysis for zero-point energy (ZPE) correction. The energies discussed here are the sum of electronic and thermal energies at 298 K. The DFT optimized structures were shown by Gauss View (version 3.07) software.

Results and discussion

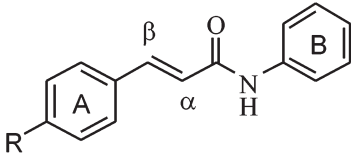
The structures of the *N*-phenylcinnamides studied are listed in Table 1 and all the compounds gave similar fragmentation in the MS/MS experiments. As an example, Fig. 1 shows the CID mass spectrum for prototype *N*-phenylcinnamide (compound 1).

Abundant product ions were observed and their formation could be rationalized by the proposed mechanism depicted in Scheme 1. The accurate mass measurement of the product ions were performed by FTICR-MS/MS and the elemental compositions of these ions were confirmed with a high degree of confidence (Table 2).

Reactive intermediates resulting from dissociative protonation

The *N*-phenylcinnamides studied have multiple protonation sites, including carbonyl oxygen, amide nitrogen atom, either carbon of the vinyl unit, the phenyl rings, and the substituent when it has a heteroatom. The structures containing different protonation sites of compound 1 were optimized at the RB3LYP/6-31G(d) level and the relative energies of these structures are summarized in Table 3. Overall, the computation results indicate that the carbonyl oxygen is the most thermodynamically favored protonation site and it gives rise to the **MH-1** ion as described in Scheme 1.

Table 1 Relative abundances of product ions in the CID spectra of $[M + H]^+$ ions of *N*-phenylcinnamides (excitation amplitude was 0.50 V)

Compound	R									
		$[M + H]^+$	$C_{13}H_{11}NR^+$	$C_9H_8ON^+$	$C_9H_6OR^+$	$C_7H_6ON^+$	$C_8H_8R^+$	$C_8H_6R^+$	$C_6H_8N^+$	$C_6H_5^+$
1	H	224 (8.9) ^a	182 (4.7)	146 (9.3)	131 (100)	120 (2.5)	105 (2.9)	103 (5.4)	94 (37.9)	77 (2.6)
2	N(CH ₃) ₂	267 (3.6)	225 (0.2)	146 (0.2)	174 (100)	120 (0.01)	148 (1.5)	146 (0.2)	94 (0.01)	–
3	OCH ₃	254 (14)	212 (1.0)	146 (0.8)	161 (100)	120 (1.1)	135 (4.8)	133 (0.7)	94 (1.8)	77 (0.1)
4	CH ₃	238 (12.4)	196 (2.2)	146 (5.1)	145 (100)	120 (0.7)	119 (5.5)	117 (4.4)	94 (14.7)	77 (0.7)
5	F	242 (25.2)	200 (3.7)	146 (8.3)	149 (100)	120 (4.4)	123 (3.7)	121 (2.5)	94 (48.4)	77 (3.2)
6	Cl	258 (81.3)	216 (4.3)	146 (10.1)	165 (100)	120 (4.6)	139 (4.1)	137 (1.1)	94 (49.5)	77 (2.9)
7	Br	302 (100)	260 (0.9)	146 (2.3)	209 (20.5)	120 (0.8)	183 (0.5)	181 (0.03)	94 (8.2)	77 (0.5)
8	CF ₃	292 (100)	250 (3.4)	146 (1.0)	199 (19.2)	120 (1.6)	173 (0.05)	171 (0.1)	94 (11.2)	77 (0.8)

^a *m/z* (relative abundance, %).

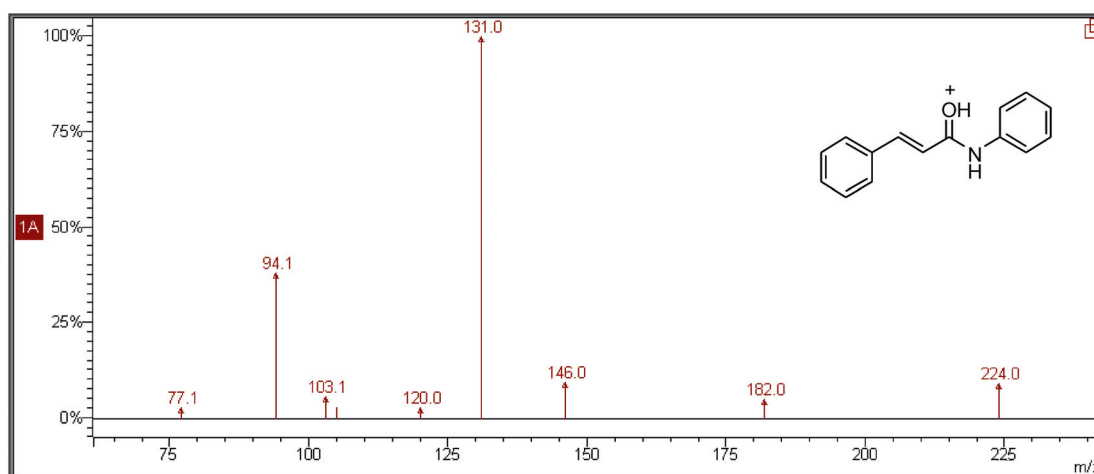
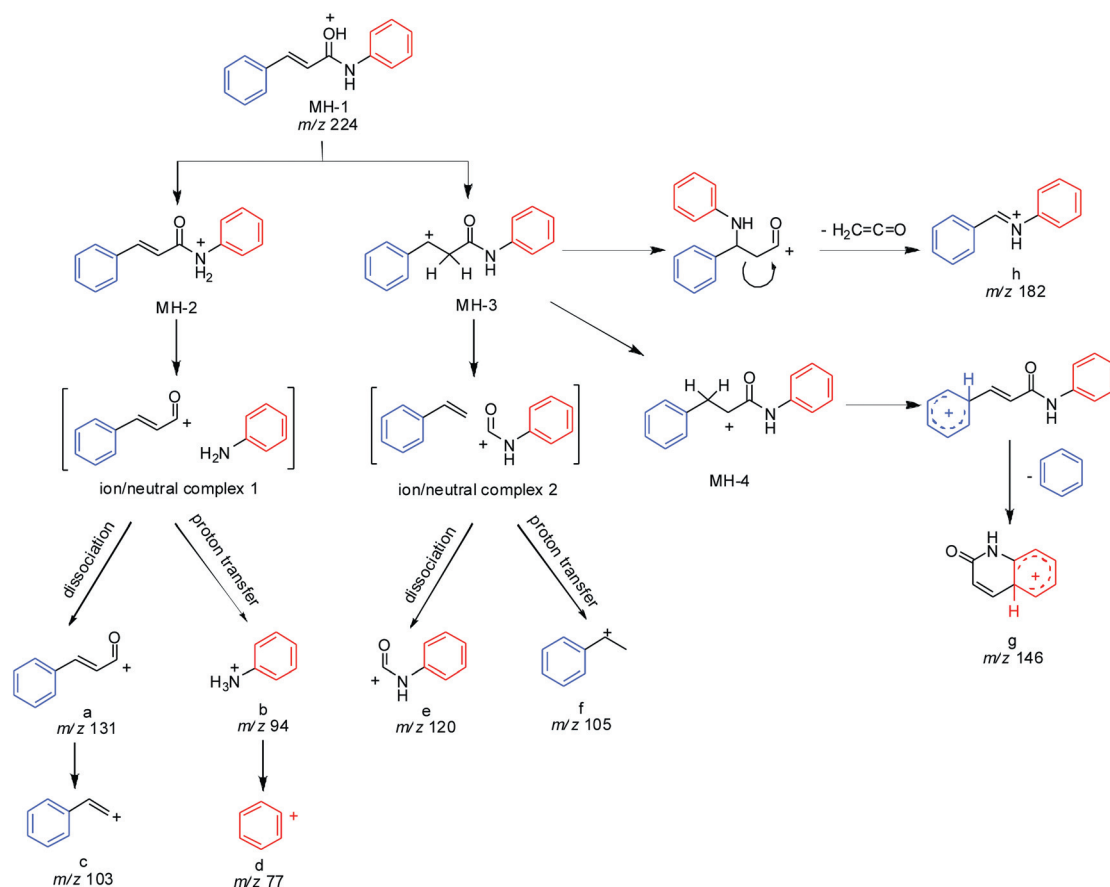


Fig. 1 CID mass spectrum of the $[M + H]^+$ ion (*m/z* 224) of *N*-phenylcinnamide.



Scheme 1 Proposed fragmentation mechanism of protonated *N*-phenylcinnamide.

Table 2 Accurate masses of product ions in the fragmentation of the $[M + H]^+$ ion of compound **1**

Measured mass	Calculated mass	Error (ppm)	Elemental composition
224.1069	224.1070	−0.4	C ₁₅ H ₁₄ ON
182.0965	182.0964	0.5	C ₁₃ H ₁₂ N
146.0600	146.0600	0.0	C ₉ H ₈ ON
131.0491	131.0491	0.0	C ₉ H ₇ O
120.0445	120.0444	0.8	C ₇ H ₆ ON
105.0698	105.0699	−1.0	C ₈ H ₉
103.0542	103.0542	0.0	C ₈ H ₇
94.0651	94.0651	0.0	C ₆ H ₈ N
77.0385	77.0386	−1.3	C ₆ H ₅

Table 3 Relative energies of structures with different protonation sites of compound **1**

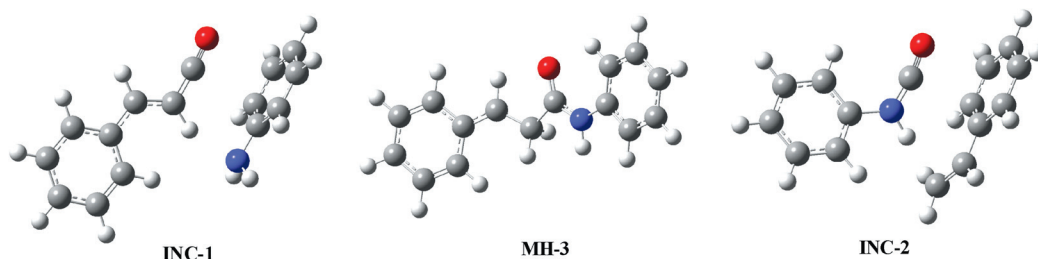
Site of protonation	Relative energy (kcal mol ^{−1})
Carbonyl oxygen	0.0
Nitrogen	13.9
α-Carbon	19.5
<i>ipso</i> -Position of phenyl ring A	32.1
<i>ipso</i> -Position of phenyl ring B	39.9

However, for the subsequent fragmentation, the proton has to transfer from the carbonyl oxygen to other less favored sites

such as the amide nitrogen atom and the α-carbon atom which were described previously as the dissociative protonation sites.^{14,15} When the proton migrates to the amide nitrogen atom (MH-2), the n-π conjugation of the lone pair electrons on the nitrogen atom to the carbonyl group is destroyed, which makes the C–N bond facile to rupture, leading to the formation of a reactive intermediate ion/neutral complex 1 (INC-1), [Ph–CH=CH–CO⁺/aniline]. In the case of migration of the proton to the α-carbon atom, another important intermediate MH-3 is formed. Direct cleavage of the bond between the α-carbon atom and the carbonyl carbon induced by the positive charge in MH-3 results in the formation of reactive intermediate ion/neutral complex 2 (INC-2), [Ph–NH–CO⁺/styrene]. Theoretical calculations are involved in the investigation of the fragmentation mechanisms and the DFT optimized structures of these intermediates are illustrated in Scheme 2. Many interesting reactions are mediated by these important reactive intermediates.

Proton transfer via INC-1: formation of protonated aniline

In the CID mass spectrum of compound **1**, cinnamoyl cation at *m/z* 131 (ion **a**) and protonated aniline at *m/z* 94 (ion **b**) are the two major fragment ions. The ion **a** could undergo a further loss of CO to produce ion **c** at *m/z* 103 and ion **b** further lose ammonia to form ion **d** at *m/z* 77. The fission of amide bond is one of the most typical and important reactions for amide



Scheme 2 DFT optimized structures of intermediates INC-1, MH-3 and INC-2.

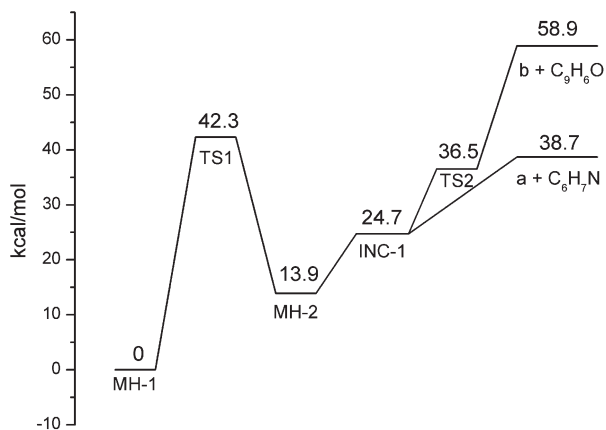


Fig. 2 Potential energy diagram for the fragmentation reactions mediated by INC-1 of compound 1, using DFT calculations at the RB3LYP/6-31G(d) level.

compounds both in solution and in the gas phase and *N*-protonation *via* a 1,3-H shift is required for the cleavage. For *N*-phenylcinnamide, the activation energy for this 1,3-H shift process *via* transition state 1 (TS1) is 42.3 kcal mol⁻¹. The cleavage of the amide bond leads to the formation of intermediate INC-1 which consists of cinnamoyl cation and neutral aniline. Due to the intense inductive effect of the positive charge, the α -hydrogen of the cinnamoyl cation is transferable.⁴⁶ Then the proton transfers *via* TS2 (36.5 kcal mol⁻¹) from the charged to the neutral partner leading to the formation of protonated aniline. A schematic potential energy surface is given in Fig. 2 to quantitatively describe the energy requirement of these reactions.

Isotopic labeling is a powerful tool for the study of reaction mechanisms so D-labeling experiments were carried out. In the CID mass spectrum of [M + D]⁺ ion of compound 1 (Fig. S1†), the ions at *m/z* 132 and 95 were observed besides the ions at *m/z* 131 and 94, and also the ions resulting from the further losses at *m/z* 104, 103, 78 and 77 were observed. This indicates that the H/D exchange reactions between the external deuterium and the amide hydrogen, vinyl hydrogens and even the hydrogens of the phenyl rings took place and the proton was floating in the molecular ion.^{15,18,47–52} The proposed mechanism was shown in Scheme S1.†

As suggested in Scheme 1, ion **a** results from the dissociation of the intermediate INC-1 and ion **b** arises from the proton transfer reaction within the complex. The fragmentation mechanisms could be further explored by studying the substituent effects on these two competitive reactions and the spectra of a series of

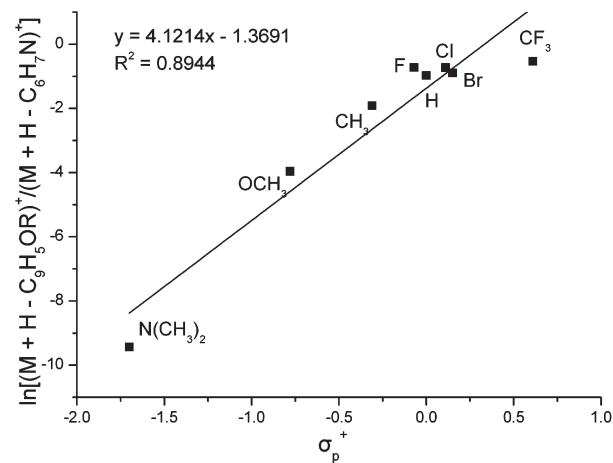


Fig. 3 Plot of $\ln[(M + H - C_9H_5OR)^+/(M + H - C_6H_7N)^+]$ vs. the σ_p^+ substituent constants for the CID reactions of the [M + H]⁺ ions of *N*-phenylcinnamides monosubstituted at the *para* position. Collision energy was 0.50 V (helium).

compounds with different substituents at the *para* position of the A-ring were measured (the RAs of the ions are shown in Table 1). A plot of abundance ratio of these two ions, $\ln[(M + H - C_9H_5OR)^+/(M + H - C_6H_7N)^+]$ versus the substituent constants, σ_p^+ , was obtained as illustrated in Fig. 3. The trend clearly indicates that the electron-donating substituents favored dissociation of the complex to form the cinnamoyl cation, whereas the electron-withdrawing groups favored the formation of protonated aniline through the proton transfer reaction within the complex. For compounds with electron-donating groups, the substituted cinnamoyl cation is stabilized by delocalization of the positive charge over the aromatic ring. This indicates that the dissociation of the complex (aniline loss) is more favorable relative to compound 1. In contrast, for compounds with electron-withdrawing groups, the electropositivity of the phenyl ring is increased and the α -hydrogen of the cinnamoyl cation is more active since the positive charge in the substituted cinnamoyl cation is destabilized. Consequently, the proton transfer reaction within the INC-1 is more favored than for compound 1.

Proton transfer *via* INC-2: loss of phenyl isocyanate

When the proton migrates from the thermodynamically favored carbonyl oxygen to another dissociative protonation site at the α -carbon *via* TS3 (47.0 kcal mol⁻¹), another important

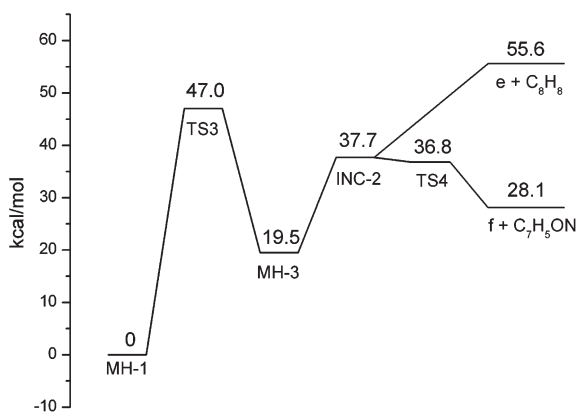


Fig. 4 Potential energy diagram for the fragmentation reactions mediated by **INC-2** of compound **1**, using DFT calculations at the RB3LYP/6-31G(d) level.

intermediate **MH-3** is formed. The cleavage of the C_{α} -CONHPh bond induced by the positive charge leads to the formation of ion/neutral complex **2** (**INC-2**), [Ph-NH-CO⁺/styrene]. In our previous studies of protonated chalcones¹⁵ and enaminones,¹⁸ the fission of the bond between the α -carbon and the carbonyl carbon results in the formation of benzoyl cation. However, in the case of *N*-phenylcinnamide, besides the dissociation of the **INC-2** to form ion **e** at m/z 120, the proton transfer reaction *via* TS4 (36.8 kcal mol⁻¹) takes place within the complex because of the existence of active amide hydrogen, leading to the formation of ion **f** at m/z 105, corresponding to the loss of phenyl isocyanate. A schematic potential energy surface for these reactions is given in Fig. 4. In the CID mass spectrum of $[M + D]^+$ ion of compound **1** (Fig. S1†), as expected, the ions at m/z 121, 120, 106 and 105 were observed. Especially, the formation of ion at m/z 105 ($C_8H_9^+$) is indisputable evidence of migration of the deuteron to the *N*-linked phenyl ring. Their formation is proposed to occur by the mechanism illustrated in Scheme S2.†

To study the influence of the substituents on the distribution of the product ions resulting from these two competitive reactions, another plot of the abundance ratio of these two ions, $\ln[(M + H - C_7H_5ON)^+/(M + H - C_8H_7R)^+]$ versus the substituent constants, σ_p^+ , was obtained (Fig. 5). Compared to the result shown in Fig. 3, the trend is the opposite. The electron-donating substituents favored the proton transfer reaction to lose phenyl isocyanate, whereas the electron-attracting substituents were in favor of the dissociation of the complex leading to the loss of styrene. For compounds with electron-donating groups, *e.g.*, compound **4** ($R = CH_3$), the PA^6 value of p -CH₃C₆H₅CH=CH₂ is 206.1 kcal mol⁻¹ which is higher than that of C₆H₅CH=CH₂ (200.8 kcal mol⁻¹). This implies that p -CH₃C₆H₅CH=CH₂ more readily accepts a proton than styrene. Besides, the product ion is more stable because the positive charge can be delocalized into the CH₃-substituted aromatic ring. These indicate that the proton transfer reaction within **INC-2** is more favorable for compound **4** relative to compound **1**. In contrast, compounds with electron-withdrawing groups, *e.g.*, compound **7** ($R = Br$), the PA value of p -BrC₆H₅CH=CH₂ (200.6 kcal mol⁻¹) is lower than that of C₆H₅CH=CH₂ and the electron-withdrawing substituent destabilized the product ion. Consequently, the proton transfer

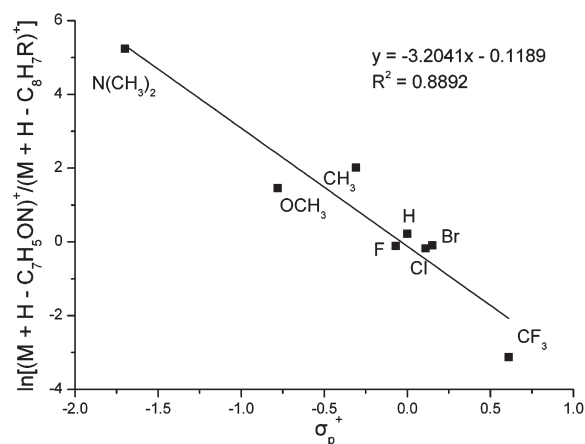


Fig. 5 Plot of $\ln[(M + H - C_7H_5ON)^+/(M + H - C_8H_7R)^+]$ vs. the σ_p^+ substituent constants for the CID reactions of the $[M + H]^+$ ions of *N*-phenylcinnamides monosubstituted at the *para* position. Collision energy was 0.50 V (helium).

reaction within the **INC-2** is less favorable for compound **7** than for compound **1**.

Stepwise proton transfer *via* **MH-3**: loss of aromatic A-ring

In the CID mass spectrum of prototype *N*-phenylcinnamide (Fig. 1), the ion **g** at m/z 146 was 78 Da less than the precursor ion. And in the CID mass spectra of other substituted *N*-phenylcinnamides, the ion resulting from loss of 78 Da was not observed whereas the ion at m/z 146 still existed. This indicates that the ion **g** arises from the loss of the aromatic A-ring rather than B-ring. As expected, in the CID mass spectrum of $[M + D]^+$ ion of compound **1** (Fig. S1†), fragment ions at m/z 147 and 146 were both observed, corresponding to loss of C₆H₆ and C₆H₅D, respectively. Their formation is rationalized by the proposed mechanism shown in Scheme S3.†

The formation of ion **g** requires the *ipso*-position of the phenyl A-ring to be protonated. In **MH-1**, the added proton can hardly transfer to the *ipso*- or *ortho*-positions directly *via* 1,5-H shift or 1,6-H shift because of the long distance and the space resistance. However, in the intermediate **MH-3**, the proton may reach the *ipso*-position of the phenyl A-ring through several pathways. The proton transfers from the α -carbon to the β -carbon through TS5, leading to the formation of **MH-4**, then the proton transfers from the β -carbon to the *ipso*-position through TS6 resulting in the loss of benzene and the formation of ion **g**. The activation barriers of these two 1,2-H shift processes are 44.7 kcal mol⁻¹ and 57.9 kcal mol⁻¹, respectively. The formation of **MH-4** may result from **MH-1**, which means the proton transfers from the carbonyl oxygen to the β -carbon *via* a 1,4-H shift through TS7. However, the energy of TS7 (51.1 kcal mol⁻¹) is higher than that of TS3 (47.0 kcal mol⁻¹) and TS5 (44.7 kcal mol⁻¹). This implies the reaction of losing the phenyl A-ring is mediated by **MH-3**. Alternatively, in **MH-3**, the proton may transfer from the α -carbon to one of the *ortho*-positions leading to the formation of **MH-5** through a five-membered-ring TS8 first, and then the proton could migrate from the *ortho*-position to the *ipso*-position through TS9, leading to

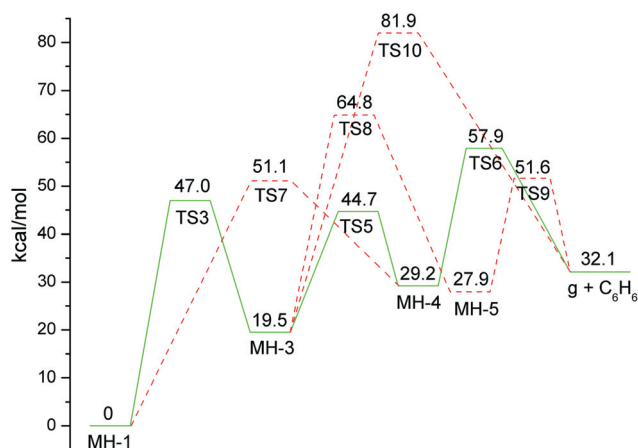


Fig. 6 Potential energy diagram for the proton transfer reactions mediated by **MH-3** to lose the phenyl A-ring of compound **1**, using DFT calculations at the RB3LYP/6-31G(d) level.

the formation of the ion **g**. The activation barriers of the 1,4-H shift and the 1,2-H shift processes are $64.8 \text{ kcal mol}^{-1}$ and $51.6 \text{ kcal mol}^{-1}$, respectively. Also the proton may migrate from the α -carbon to the *ipso*-position directly through a four-membered-ring TS10 and the energy barrier of this 1,3-H shift process is $81.9 \text{ kcal mol}^{-1}$. However, the energies of TS8 and TS10 are higher than those of TS5 and TS6. This implies that the stepwise 1,2-H shift route is more accessible in terms of energy. A schematic potential energy diagram for these proton transfer routes is given in Fig. 6.

Intramolecular nucleophilic substitution (S_Ni) via **MH-3**: loss of ketene

Ion **h** at m/z 182 is 42 Da less than the precursor ion, and it was confirmed by FTICR-MS/MS that ion **h** resulted from C_2H_2O loss. In the chemical ionization mass spectra of α,β -unsaturated carboxylic esters,⁵³ loss of ketene was observed about three decades ago. In **MH-3**, the β -carbon atom is positively charged and the amide nitrogen, which has lone pair electrons, can be a nucleophilic group. The intramolecular nucleophilic attack of the nitrogen atom at the β -carbon atom involving the cleavage of the $C_\alpha-C_\beta$ bond via TS11 ($33.1 \text{ kcal mol}^{-1}$) leads to the loss of ketene and formation of ion **h** at m/z 182. As illustrated in Fig. S1,[†] two fragment ions at m/z 183 and 182 were also observed after H/D exchange, corresponding to the loss of C_2H_2O and C_2HDO , respectively. Their formation could be rationalized by the proposed mechanism shown in Scheme S4.[†]

Conclusions

The dissociation of protonated *N*-phenylcinnamides with different functional groups was studied by tandem mass spectrometry in combination with theoretical calculations. Upon collisional activation, the proton transfers from the carbonyl oxygen, which is the thermodynamically most favorable protonation site, to the dissociative protonation sites at the amide nitrogen atom or the α -carbon atom, leading to the formations of important

intermediates **INC-1** ($[RC_6H_4CH=CHCO^+/aniline]$), **MH-3** ($[RC_6H_4CH-CH_2CONHPh]^+$) and **INC-2** ($[PhNHCO^+/RC_6H_4-CH=CH_2]$). Many interesting reactions such as proton transfer and intramolecular nucleophilic substitution are mediated by these intermediates and the effects of substituents on these reactions were also evaluated. D-labeling experiments and DFT theoretical calculations were performed to give insights into these reaction mechanisms. The present study extends and enriches our knowledge of the important roles of reactive intermediates in the dissociation of amide compounds in the gas phase.

Acknowledgements

The authors gratefully acknowledge the financial support from the NSF of China (No: 20975092 and 21025207).

Notes and references

- 1 R. Wu and T. B. McMahon, *J. Am. Chem. Soc.*, 2007, **129**, 11312–11313.
- 2 H. Chen, L. S. Eberlin, M. Neftiu, R. Augusti and R. G. Cooks, *Angew. Chem., Int. Ed.*, 2008, **47**, 3422–3425.
- 3 P. Przybylski, K. Pyta, J. Czupryniak, B. Wicher, M. Gdaniec, T. Ossowski and B. Brzezinski, *Org. Biomol. Chem.*, 2010, **8**, 5511–5518.
- 4 J. M. Perez, H. Helten, B. Donnadieu, C. A. Reed and R. Streubel, *Angew. Chem., Int. Ed.*, 2010, **49**, 2615–2618.
- 5 C. G. Ji and J. Z. H. Zhang, *J. Am. Chem. Soc.*, 2011, **133**, 17727–17737.
- 6 E. P. L. Hunter and S. G. Lias, *J. Phys. Chem. Ref. Data*, 1998, **27**, 413–656.
- 7 Z. Tian and S. R. Kass, *J. Am. Chem. Soc.*, 2008, **130**, 10842–10843.
- 8 Z. Tian and S. R. Kass, *Angew. Chem., Int. Ed.*, 2009, **48**, 1321–1323.
- 9 J. Schmidt, M. M. Meyer, I. Spector and S. R. Kass, *J. Phys. Chem. A*, 2011, **115**, 7625–7632.
- 10 Y.-P. Tu and A. G. Harrison, *J. Am. Soc. Mass Spectrom.*, 1998, **9**, 454–462.
- 11 G. E. Reid, R. J. Simpson and R. A. J. O'Hair, *J. Am. Soc. Mass Spectrom.*, 2000, **11**, 1047–1060.
- 12 J. Zhao, T. Shoeib, K. W. M. Siu and A. C. Hopkinson, *Int. J. Mass Spectrom.*, 2006, **255/256**, 265–278.
- 13 V. H. Wysocki, G. Tsapralis, L. L. Smith and L. A. Breck, *J. Mass Spectrom.*, 2000, **35**, 1399–1406.
- 14 Y.-P. Tu, *J. Org. Chem.*, 2006, **71**, 5482–5488.
- 15 N. Hu, Y.-P. Tu, Y. Liu, K. Jiang and Y. Pan, *J. Org. Chem.*, 2008, **73**, 3369–3376.
- 16 Y. Tu, Y. Huang, C. Atsriku, Y. You and J. Cuniff, *Rapid Commun. Mass Spectrom.*, 2009, **23**, 1970–1976.
- 17 P. Liu, N. Hu, Y. Pan and Y. Tu, *J. Am. Soc. Mass Spectrom.*, 2010, **21**, 626–634.
- 18 C. Guo, J. Wan, N. Hu, K. Jiang and Y. Pan, *J. Mass Spectrom.*, 2010, **45**, 1291–1298.
- 19 K. Jiang, G. Bian, N. Hu, Y. Pan and G. Lai, *Int. J. Mass Spectrom.*, 2010, **291**, 17–23.
- 20 Y. Chai, C. Guo, K. Jiang, Y. Pan and C. Sun, *Org. Biomol. Chem.*, 2012, **10**, 791–797.
- 21 T. H. Morton, *Tetrahedron*, 1982, **38**, 3195–3243.
- 22 D. J. McAdoo, *Mass Spectrom. Rev.*, 1988, **7**, 363–393.
- 23 R. D. Bowen, *Acc. Chem. Res.*, 1991, **24**, 364–371.
- 24 R. D. Bowen, A. W. Colburn and P. J. Derrick, *J. Chem. Soc., Perkin Trans. 2*, 1991, 147–151.
- 25 R. D. Bowen and P. J. Derrick, *J. Chem. Soc., Perkin Trans. 2*, 1992, 1033–1039.
- 26 T. H. Morton, *Org. Mass Spectrom.*, 1992, **27**, 353–368.
- 27 P. Longevialle, *Mass Spectrom. Rev.*, 1992, **11**, 157–192.
- 28 R. D. Bowen, *Org. Mass Spectrom.*, 1993, **28**, 1577–1595.
- 29 R. D. Bowen, A. D. Wright and P. J. Derrick, *J. Chem. Soc., Perkin Trans. 2*, 1993, 501–507.

- 30 D. J. McAdoo and T. H. Morton, *Acc. Chem. Res.*, 1993, **26**, 295–302.
- 31 P. N. Rylander and S. Meyerson, *J. Am. Chem. Soc.*, 1956, **78**, 5799–5802.
- 32 C. L. Perrin, *Acc. Chem. Res.*, 1989, **22**, 268–275.
- 33 R. S. Brown, A. J. Bennet and H. Slebocka-Tilk, *Acc. Chem. Res.*, 1992, **25**, 481–488.
- 34 C. Cox and T. Lectka, *Acc. Chem. Res.*, 2000, **33**, 849–858.
- 35 H.-Y. Lin, D. P. Ridge, E. Uggerud and T. Vulpus, *J. Am. Chem. Soc.*, 1994, **116**, 2996–3004.
- 36 D. R. Mueller, M. Eckersley and W. J. Richter, *Org. Mass Spectrom.*, 1988, **23**, 217–222.
- 37 A. R. Dongre, J. L. Jones, A. Somogyi and V. H. Wysocki, *J. Am. Chem. Soc.*, 1996, **118**, 8365–8374.
- 38 I. P. Csonka, B. Paizs, G. Lendvay and S. Suhai, *Rapid Commun. Mass Spectrom.*, 2000, **14**, 417–431.
- 39 N. C. Polfer, J. Oomens, S. Suhai and B. Paizs, *J. Am. Chem. Soc.*, 2007, **129**, 5887–5897.
- 40 E. Daeseleire, H. De Ruyck and R. Van Renterghem, *Rapid Commun. Mass Spectrom.*, 2000, **14**, 1404–1409.
- 41 C. K. Fagerquist, A. R. Lightfield and S. J. Lehotay, *Anal. Chem.*, 2005, **77**, 1473–1482.
- 42 W. W. Bullen, R. A. Miller and R. N. Hayes, *J. Am. Soc. Mass Spectrom.*, 1999, **10**, 55–66.
- 43 M. Jemal, Z. Ouyang, B. C. Chen and D. Teitz, *Rapid Commun. Mass Spectrom.*, 1999, **13**, 1003–1015.
- 44 B. J. Leslie, C. R. Holaday, T. Nguyen and P. J. Hergenrother, *J. Med. Chem.*, 2010, **53**, 3964–3972.
- 45 G. W. Frisc, H. B. Schlegel, G. E. Scuseria, M. A. Robb, J. R. Cheeseman, V. G. Zakrzewski, J. A. Montgomery, R. E. Stratmann, J. C. Burant, S. Dapprich, J. M. Millam, A. D. Daniels, K. N. Kudin, M. C. Strain, O. Farkas, J. Tomasi, V. Barone, M. Cossi, R. Cammi, B. Mennucci, C. Pomelli, C. Adamo, S. Clifford, J. Ochterski, G. A. Petersson, P. Y. Ayala, Q. Cui, K. Morokuma, D. K. Malick, A. D. Rabuck, K. Raghavachari, J. B. Foresman, J. Cioslowski, J. V. Ortiz, B. B. Stefanov, G. Liu, A. Liashenko, P. Piskorz, I. Komaromi, R. Gomperts, R. L. Martin, D. J. Fox, T. Keith, M. A. Al-Laham, C. Y. Peng, A. Nanayakkara, C. Gonzalez, M. Challacombe, P. M. W. Gill, B. Johnson, W. Chen, M. W. Wong, J. L. Andres, C. Gonzalez, M. E. Head-Gordon, S. Replogle and J. A. Pople, *GAUSSIAN 03*, Gaussian, Inc., Pittsburgh, PA, 2003.
- 46 C. Guo, N. Hu, K. Jiang, W. Chen, X. Wang and Y. Pan, *Rapid Commun. Mass Spectrom.*, 2010, **24**, 409–414.
- 47 U. Filges and H. F. Grutzmacher, *Org. Mass Spectrom.*, 1986, **21**, 673–680.
- 48 U. Filges and H. F. Grutzmacher, *Org. Mass Spectrom.*, 1987, **22**, 444–450.
- 49 H. F. Grutzmacher and G. Thielking, *Org. Mass Spectrom.*, 1988, **23**, 397–405.
- 50 G. Thielking, U. Filges and H. F. Grutzmacher, *J. Am. Soc. Mass Spectrom.*, 1992, **3**, 417–426.
- 51 D. Kuck, *J. Labelled Compd. Radiopharm.*, 2007, **50**, 360–365.
- 52 C. Guo, Y. Zhou, P. Liu, Y. Chai and Y. Pan, *J. Am. Soc. Mass Spectrom.*, 2012, **23**, 1191–1201.
- 53 A. G. Harrison and H. Ichikawa, *Org. Mass Spectrom.*, 1980, **15**, 244–248.